Spectrally Enhancing Near-Field Radiative Transfer between Metallic Gratings by Exciting Magnetic Polaritons in Nanometric Vacuum Gaps

Yue Yang[1] and Liping Wang[1,*]

School for Engineering of Matter, Transport, and Energy, Arizona State University, Tempe, Arizona 85287, USA

(Received 31 October 2015; published 21 July 2016)

In the present Letter, we theoretically demonstrate that near-field radiative transport between one-dimensional periodic grating microstructures separated by nanometer vacuum gaps can be spectrally enhanced by exciting magnetic polaritons. Fluctuational electrodynamics that incorporates scattering matrix theory with rigorous coupled-wave analysis is employed to exactly calculate the near-field radiative flux between two metallic gratings. In addition to the well-known coupled surface plasmon polaritons, the radiative flux can be also spectrally enhanced due to the magnetic polariton, which is excited in the gap between the grating ridges. The mechanism of magnetic polaritons in the near-field radiative transport are elucidated in detail, while the unusual enhancement cannot be predicted by either Derjaguin's or the effective medium approximations. The effects of the vacuum gap distance and grating geometry parameters between the two gratings are investigated. The findings will open a new way to spectrally control near-field radiative transfer by magnetic polaritons with micro- or nanostructured metamaterials, which holds great potential for improving the performance of energy systems like near-field thermophotovoltaics.

DOI: 10.1103/PhysRevLett.117.044301

It has been demonstrated during the last decade that radiative transfer could be significantly enhanced when the distance between two objects is smaller than the characteristic thermal wavelength due to photon tunneling or coupling of evanescent waves [1–3]. In particular, the near-field radiative flux could far exceed the blackbody limit by the resonant coupling of surface plasmon polaritons (SPPs) or surface phonon polaritons (SPhPs) across the vacuum gap both theoretically and experimentally [4,5]. Recently, excitations of magnetic SPhPs [6,7], hyperbolic modes [8–10], and epsilon-near-pole or epsilon-near-zero modes [11] with different types of metamaterials have also been studied to further improve the near-field radiative flux. Moreover, compared to the case of two plates, the near-field radiative transport between two gratings can be further enhanced due to guided modes [12] and spoof surface plasmon polaritons [13] between two Au gratings at a large vacuum gap distance of 1 μm, and hyperbolic modes between two doped silicon gratings [14]. Near-field thermal radiation could find many promising applications in energy harvesting [1,15], near-field imaging [16], and thermal management [17–22]. Several experimental methods have been reported to measure the near-field radiative heat flux between planar surfaces at submicron vacuum gaps [23–25].

Magnetic polaritons (MPs) refer to the strong coupling of external electromagnetic waves with the magnetic resonance excited inside the nanostructures. MPs artificially realized with metallic micro- or nanostructures have been employed to control light propagation and tailor exotic optical and radiative properties in the far field, such as selective solar absorbers [26], thermophotovoltaic emitters [27], and switchable or tunable metamaterials [28,29]. Phonon-mediated MPs have also been excited in both SiC deep grating and binary grating configurations [30,31]. On the other hand, MP excitation has been achieved in the SiO_2 spacer between two Ag binary gratings [32]. In comparison to SPPs or SPhPs that have been well studied for tailoring both far- and near-field thermal radiation, magnetic resonance or MPs have only been investigated for controlling far-field thermal radiation, while their role in near-field radiative transport has yet to be identified. In this Letter, we will theoretically investigate the possible effect of MPs in the near-field radiative transfer between two metallic grating microstructures separated by a vacuum gap d below 100 nm.

As depicted in Fig. 1(a), the gratings are assumed to be perfectly aligned with period, depth, and ridge width, respectively, as $\Lambda = 2$ μm, $h = 1$ μm, and $w = 1$ μm, which are kept unchanged in the present work unless specified. Vacuum is considered to be in the grating grooves, while the metal filling ratio is then $f = w/\Lambda = 0.5$. The temperatures of the emitter and receiver are set as T_h and T_l, respectively. Note that an equivalent inductor-capacitor (LC) circuit model, which has been widely used to predict the MP resonance frequency in the far field [32], is also shown in Fig. 1(a) along with the resulting current loop. The question is that whether MP resonance can be excited in the nanometer vacuum gap to spectrally enhance near-field radiative transfer. To address this question, the scattering formalism [33–35] that is incorporated into fluctuational electrodynamics with rigorous coupled-wave analysis (RCWA) [36,37] is employed to rigorously calculate the near-field radiative flux. The dielectric function of the metals is described by a Drude model as $\varepsilon_{\text{Drude}}(\omega) = 1 - [\omega_p^2/(\omega^2 + i\gamma\omega)]$, where ω is the angular frequency, the plasma frequency is $\omega_p = 1.37 \times 10^{16}$ rad/s, and the scattering rate

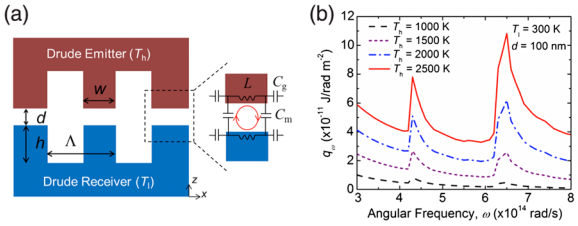

FIG. 1. (a) Schematic of the radiative transfer between two symmetric, perfectly aligned metallic gratings with parameters of period ($\Lambda = 2$ μm), depth ($h = 1$ μm), and ridge width ($w = 1$ μm). The Drude emitter and receiver temperatures are, respectively, set as T_h and T_l. The vacuum gap distance is denoted as d. An equivalent LC circuit model and the resulting electrical current loops in the vacuum gap at the excitation of the MP are also depicted. (b) Spectral heat fluxes between these two perfectly aligned metallic gratings at different emitter temperatures when the receiver is separated by a vacuum gap of $d = 100$ nm and maintained at $T_l = 300$ K.

is $\gamma = 7.31 \times 10^{13}$ rad/s [38], which are taken from the material properties of gold at room temperature as an example here. While the present study mainly focuses on the explanation of the physical mechanism and behavior of MP resonance in the near-field radiative transfer, similar MP excitation is expected to occur with other metals like Ag, Al, and W [26,27,32], as well as some refractory plasmonic materials like ITO, AZO, and TiN, which could possibly withstand high temperatures up to 3250 K [11].

Through the exact scattering theory, near-field spectral radiative transfer between two gratings is expressed as [39,40]

$$q_\omega = \frac{1}{2\pi^3}[\Theta_h(\omega, T_h) - \Theta_l(\omega, T_l)] \times \int_0^{\pi/\Lambda}\int_0^{\infty} \xi(\omega, k_{x0}, k_y) dk_y dk_{x0}, \quad (1)$$

where $\Theta(\omega, T) = \hbar\omega/(e^{\hbar\omega/k_B T} - 1)$ is the Planck oscillator, and k_{x0} and k_y are the incident wave vector components at the grating surface in the x and y directions, respectively. The energy transmission coefficient $\xi(\omega, k_{x0}, k_y)$, which considers all the polarization states, is

$$\xi(\omega, k_{x0}, k_y) = \mathrm{tr}(\mathbf{D}\mathbf{W}_1\mathbf{D}^\dagger\mathbf{W}_2), \quad (2a)$$

$$\mathbf{D} = (\mathbf{I} - \mathbf{S}_1\mathbf{S}_2)^{-1}, \quad (2b)$$

$$\mathbf{W}_1 = \Sigma_{-1}^{p\omega} - \mathbf{S}_1\Sigma_{-1}^{p\omega}\mathbf{S}_1^\dagger + \mathbf{S}_1\Sigma_{-1}^{e\omega} - \Sigma_{-1}^{e\omega}\mathbf{S}_1^\dagger \quad (2c)$$

$$\mathbf{W}_2 = \Sigma_1^{p\omega} - \mathbf{S}_2^\dagger\Sigma_1^{p\omega}\mathbf{S}_2 + \mathbf{S}_2^\dagger\Sigma_1^{e\omega} - \Sigma_1^{e\omega}\mathbf{S}_2, \quad (2d)$$

where $\mathbf{D}$ is the so-called Fabry-Perot denominator considering the multiple reflection between two gratings, $\mathbf{W}_i$ indicates the photon absorption, $\mathbf{S}_1 = \mathbf{R}_1$, and $\mathbf{S}_2 = e^{ik_{z0}d}\mathbf{R}_2 e^{ik_{z0}d}$. $\mathbf{R}_1$ and $\mathbf{R}_2$ are the reflection operators of the two gratings, which can be obtained through the RCWA method [36,37,41]. $k_x^{(n)} = k_{x0} + n(2\pi/\Lambda)$ is defined according to the Bloch wave condition. n runs from $-N$ to N, where N is the highest diffraction order. The operators $\Sigma_n^{p\omega/e\omega} = \frac{1}{2}k_z^n\Pi^{p\omega/e\omega}$, where $\Pi^{p\omega/e\omega}$ are the projectors on the propagative and evanescent sectors, were clearly defined in Ref. [39]. The details on the numerical convergence can be found in the Supplemental Material [42], while our algorithm was validated by comparison with other works [12,43] [see Figs. S1 and S2(a) in the Supplemental Material [42]]. The results obtained by the scattering matrix theory are treated to be rigorous.

Figure 1(b) presents the spectral heat fluxes between two metallic gratings at a vacuum gap distance of $d = 100$ nm with different emitter temperatures T_h from 1000 to 2500 K when the receiver temperature is fixed at $T_l = 300$ K. There clearly exist two spectral heat flux peaks around the angular frequencies of 4.3×10^{14} rad/s and 6.5×10^{14} rad/s. As T_h increases, the spectral peak locations surprisingly do not change, while the peak amplitudes are greatly enhanced mainly due to a more energetic Planck oscillator at higher temperatures. For example, the spectral heat flux q_ω at the frequency of 6.5×10^{14} rad/s could reach as high as 1.1×10^{-10} J/rad m^{-2} at $T_h = 2500$ K. Note that the angular frequency of 6.5×10^{14} rad/s corresponds to 0.43 eV in energy; thus, the observed spectral heat flux peaks could possibly greatly improve the thermophotovoltaic (TPV) energy conversion by spectrally enhancing photon transport above the band gaps of the TPV cells (e.g., $In_xGa_{1-x}As$ with band gaps varying from 0.36 to 1.42 eV).

In order to understand the physical mechanisms responsible for these two spectral heat flux peaks, we first investigate the spectral heat fluxes at different vacuum gap distances of $d = 100$, 50, 20, and 10 nm as shown in Fig. 2. As the Planck oscillator only considers the effect of the temperature, the spectral heat flux q_ω is normalized to the Planck oscillator difference $\Theta_h - \Theta_l$ in order to directly indicate the effects of the materials and structures on the radiative transfer, which would better reveal the underlying mechanisms. It can be clearly observed from Fig. 2(a) that at a vacuum gap distance of $d = 100$ nm, there are two peaks of normalized spectral heat flux at angular frequencies of 4.3×10^{14} rad/s and 6.5×10^{14} rad/s, respectively. When d decreases to 50 nm, the larger peak shifts to $\omega = 6.0 \times 10^{14}$ rad/s and further to 5×10^{14} rad/s at $d = 20$ nm. However, when d becomes 10 nm, there are two spectral peaks, respectively, at the frequencies of 4×10^{14} rad/s and 7.8×10^{14} rad/s in addition to the small spectral peak around $\omega = 4.3 \times 10^{14}$ rad/s, whose frequency does not change at all at different vacuum gaps, but the peak amplitude increases from 0.5×10^{10} rad^{-1} m^{-2} at $d = 100$ nm to 1×10^{11} rad^{-1} m^{-2} at $d = 10$ nm.

In order to understand the physical mechanisms responsible for the normalized spectral heat flux peaks predicted by the rigorous calculation, Derjaguin's proximity approximation (PA) method is first considered, which represents a weighted approach for SPhP or SPP coupling with different vacuum gap distances. The spectral heat flux between the two gratings from the PA method can be weighted by the ones between two plates with different gap distances as

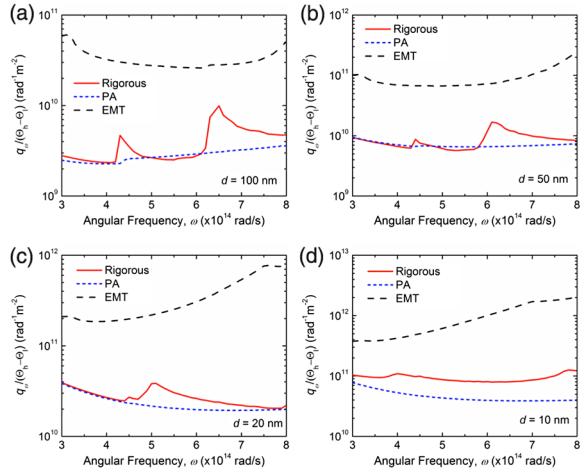

FIG. 2. Normalized spectral heat fluxes between the Drude grating emitter and receiver at different vacuum gaps of (a) $d = 100$ nm, (b) $d = 50$ nm, (c) $d = 20$ nm, and (d) $d = 10$ nm obtained from the scattering matrix method (denoted as "rigorous") in comparison with those from Derjaguin's proximity approximation method (denoted as "PA") and effective medium theory (denoted as "EMT").

$$q_\omega^{\mathrm{PA}} = f \times q_\omega^{\mathrm{plate}}(d) + (1-f) \times q_\omega^{\mathrm{plate}}(d+2h), \quad (3)$$

where $q_\omega^{\mathrm{plate}}(L)$ is the spectral heat flux between the two plates with a gap distance L. As inferred by Eq. (3), the PA method only considers the contributions by SPP coupling between the planar surfaces at different vacuum gap distances. This indicates that the PA method would be accurate if coupled SPhP or SPP resonance is the only mechanism that dominates near-field radiative transfer (see Fig. S2 in the Supplemental Material [42]). However, by comparing the normalized spectral heat flux from the PA method to the rigorous solution in Fig. 2, the PA method turns out to be accurate with good agreement with the rigorous solution except for the angular frequencies where spectral heat flux peaks exist for d from 100 to 20 nm. At $d = 10$ nm, the PA method fails to predict the exact values by significant discrepancies within the entire spectrum of interest. Apparently, the PA method or the SPP coupling between the planar surfaces cannot explain the spectral heat flux peaks that exist between the metallic gratings.

Furthermore, the effective medium theory (EMT), which considers the grating layer as a homogeneous uniaxial medium, is also examined to determine whether or not is it responsible for the spectral enhancement. By setting the diffraction order to zero in the RCWA algorithm, the metallic gratings are considered as effectively homogenous media with zero-order approximation (see Figs. S3 and S4 in the Supplemental Material [42]). The near-field radiative flux between the metallic gratings with effective media approximation was also calculated and presented in Fig. 2 with different vacuum gaps. Compared with the rigorous method, the EMT method overpredicts the normalized spectral heat flux by one order of magnitude, which is due to the enhancement from the hyperbolic modes unnecessarily predicted by the effective medium treatment (see the Supplemental Material [42]). After all, the EMT is inherently a homogenization approach which cannot take into account the local resonance modes like coupled SPPs or MPs that could possibly occur within the vacuum gap [14,44,45]. Therefore, effective medium approximation cannot explain the unusual radiative transfer between the metallic gratings across ultrasmall vacuum gaps, while physical mechanisms other than coupled SPPs or EMT have to be identified and understood.

To gain a better understanding of the radiative transfer between the Drude grating emitter and receiver, the contour plots of the transmission coefficient in the ω-k_{x0} domain under $k_y = 0$ from the rigorous method are presented in Fig. 3 at corresponding vacuum gap distances. Multiple bright horizontal bands, which are independent of k_{x0} and indicate the enhanced near-field radiative transfer channels, can be clearly observed. Among the different vacuum gap distances, the one at $\omega = 4.3 \times 10^{14}$ rad/s barely shifts with different d values, which corresponds to the smaller spectral heat flux peak at the same frequency observed in Fig. 2. As intensively discussed in Ref. [12], this is associated with the guided mode, whose resonance condition strongly depends on the cavity depth, i.e., $H = 2h + d$. Note that the grating depth is $h = 1$ μm, which is much larger than the sub-100-nm vacuum gap distances considered here. Therefore, it can be understood that the guide mode would not shift when d varies from 100 to 10 nm as $H \gg d$. However, the same theory of guided modes cannot explain the brighter and broader resonance mode around $\omega = 6.5 \times 10^{14}$ rad/s at $d = 100$ nm, which clearly shifts to lower frequencies with smaller d. As the coupled SPPs, effective medium, and guided modes cannot explain this particular unusual spectral enhancement between the metallic gratings, could it be associated with a possible excitation of the magnetic resonance or MP?

In order to verify our hypothesis of the MP resonance, an equivalent LC circuit is employed to analytically predict the resonance conditions of the MP between two metallic gratings in the near field [32]. Note that the LC model based on the resonant charge distributions has been successfully employed to verify the physical mechanisms of MP modes in metal-insulator-metal (MIM) nanostructures in selective control of far-field thermal radiation [29–32]. After all, the nanometer vacuum gap between the Drude grating emitter and receiver here forms similar MIM configurations (see Fig. S5 in the Supplemental Material [42]). Here, the inductance of the metallic gratings can be expressed as $L = L_m + L_e$, where the first term $L_m = 0.5\ \mu_0 wd$ accounts for the mutual inductance of two parallel plates with width w separated by a distance d, and the kinetic inductance $L_e = \omega/(\varepsilon_0 \omega_p^2 \delta)$ considers the contribution of drifting electrons. Note that μ_0 and ε_0 are the permeability and permittivity of vacuum, while $\delta = \lambda/2\pi\kappa$ is the field penetration depth with κ being the extinction coefficient of the metal. On the other hand, the parallel-plate capacitance between the upper and

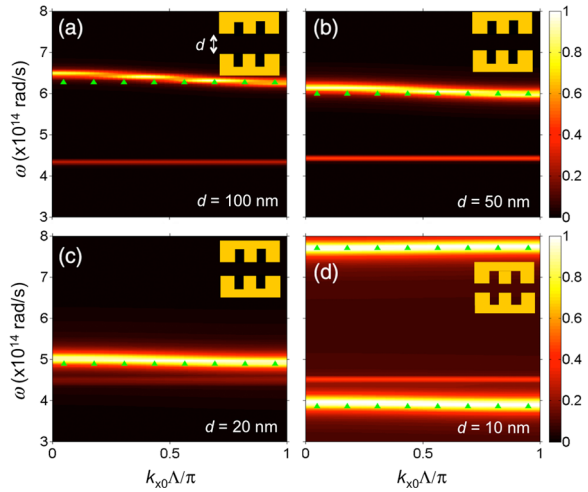

FIG. 3. Contour plots of energy transmission coefficient (ξ) between the Drude grating emitter and receiver at vacuum gaps of (a) $d = 100$ nm, (b) $d = 50$ nm, (c) $d = 20$ nm, and (d) $d = 10$ nm. The base geometric parameters of the metallic gratings are $\Lambda = 2$ μm, $w = 1$ μm, and $h = 1$ μm. Note that $k_y = 0$ is assumed and k_{x0} is normalized to the first Brillouin zone. The LC circuit model prediction of the MP resonance conditions is shown as green triangles.

lower metal ridges can be expressed as $C_m = c_1\varepsilon_0 w/d$, where $c_1 = 0.22$ is the correction factor considering nonuniform charge distribution [32]. The capacitance between the left and right metal ridges is denoted as $C_g = \varepsilon_0 h/(\Lambda - w)$. Thus, the resonance frequency for the fundamental MP mode can be obtained when the total circuit impedance reaches zero:

$$\omega_{\mathrm{MP1}} = 1/\sqrt{(L_m + L_e)(C_m + C_g)}. \tag{4}$$

With the base grating geometries as $\Lambda = 2$ μm, $w = 1$ μm, $h = 1$ μm, the MP1 resonance frequencies between the Drude grating emitter and receiver are predicted to be 6.4×10^{14} rad/s, 6.0×10^{14} rad/s, 4.9×10^{14} rad/s, and 3.8×10^{14} rad/s, respectively, for $d = 100$, 50, 20, and 10 nm, which match surprisingly well with the unusual spectral enhancement mode predicted by the rigorous solution as shown in Fig. 3. Note that the independence of the MP resonance condition on k_{x0} has been thoroughly discussed and well understood previously [31,32]. At $d = 10$ nm, the contour shows an additional resonance mode around $\omega = 7.7 \times 10^{14}$ rad/s, which is actually the second harmonic order of the MP resonance with doubled resonance frequency from MP1. The unanimous agreements between the rigorous solution and the analytical LC model prediction at different vacuum gaps clearly verify the physical mechanism of MP excitation in spectrally enhancing near-field radiative transfer between metallic grating structures.

To further confirm and understand the behaviors of MP resonance in near-field radiative transport across nanometer vacuum gaps, the grating geometric effect on the near-field radiative transfer between the Drude grating emitter and receiver is investigated in terms of the transmission coefficient at the gap distance $d = 20$ nm. Figures 4(a) and 4(b) present the effect of the grating depth, respectively, with $h = 0.5$ μm and 1.5 μm, while other geometric parameters are kept at the base values. In comparison with the case of $h = 1$ μm in Fig. 3(c), the strong and broad MP resonance mode around $\omega = 5 \times 10^{14}$ rad/s slightly shifts toward lower frequencies, which is in good agreement with the LC model prediction. Note that the grating depth h only affects the capacitance C_g, which is less than $C_m/10$ and thereby negligible with the given parameters. Therefore, h has little effect on the MP resonance condition. On the other hand, the guided mode, which strongly depends on the cavity depth, shifts from 4.3×10^{14} rad/s to 6.2×10^{14} rad/ when h increases from 1 to 1.5 μm.

The effect of grating width (w) on the near-field radiative transfer spectrally enhanced by the MP resonance is studied similarly in terms of the transmission coefficient. By comparing Figs. 4(c) and 4(d) with Fig. 3(c), when the grating ridges become wider from 0.8 to 1.2 μm, both the rigorous solution and the LC model consistently show that the MP resonance mode changes from $\omega = 6.1 \times 10^{14}$ rad/s to 4.2×10^{14} rad/s. From the perspective of charge distribution, the grating width (w) is linear to L_m, L_e, and C_m. With negligible C_g at $d = 20$ nm, the MP resonance frequency $\omega_{\mathrm{MP1}} \approx 1/\sqrt{(L_m + L_e)C_m}$ is essentially inversely proportional to w. Further tuning the geometric parameters of gratings, it is possible to shift the MP resonance and associated spectral flux peak to lower frequencies to better match the thermal wavelength at a given emitter temperature for the total heat flux

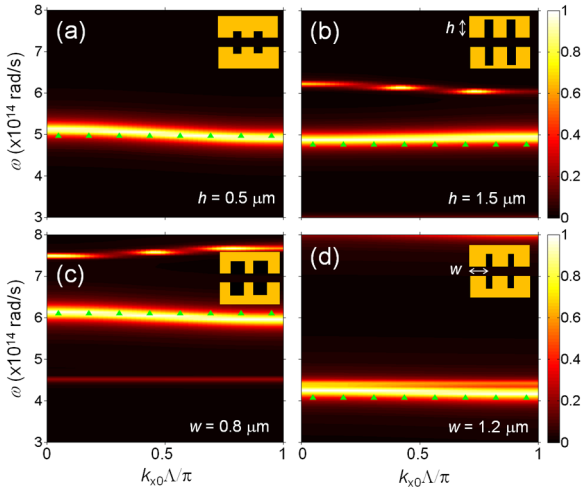

FIG. 4. Contour plots of the energy transmission coefficient (ξ) between two perfectly aligned metallic gratings at $d = 20$ nm with different geometries (a) $h = 0.5$ μm, (b) $h = 1.5$ μm, (c) $w = 0.8$ μm, and (d) $w = 1.2$ μm, while the rest of the parameters are kept at the base values $\Lambda = 2$ μm, $w = 1$ μm, and $h = 1$ μm. Note that $k_y = 0$ is assumed and k_{x0} is normalized to the first Brillouin zone. The LC circuit model prediction of the MP resonance conditions is shown as green triangles.

enhancement. However, the weaker guided mode around $\omega = 4.3 \times 10^{14}$ rad/s does not change with different a grating width, whose resonance frequency is only a strong function of cavity depth H or grating depth h [12]. In addition, the effect of the grating misalignment also confirms the consistent MP behaviors with different degrees of lateral displacement by the LC model (see Fig. S6 in the Supplemental Material [42]).

In summary, we have theoretically demonstrated an unusual spectral radiative flux enhancement between two metallic grating emitters and receivers separated by sub-100-nm vacuum gaps, which could not be explained by SPP coupling, effective medium, or guided mode. The physical mechanisms have been identified and elaborated for the first time to be the excitation of a magnetic polariton, unarguably verified by the consistency on the MP resonance modes between the rigorous solutions and the LC model predictions in terms of vacuum gap and geometric effects. The fundamental understanding gained here will open a new way to spectrally tailor near-field radiative transfer with metamaterials for thermal management and energy harvesting applications.

This work was supported by the National Science Foundation under Grant No. CBET-1454698.

*Corresponding author.
liping.wang@asu.edu

[1] S. Basu, Z. M. Zhang, and C. J. Fu, Int. J. Energy Res. **33**, 1203 (2009).
[2] D. G. Cahill, P. V. Braun, G. Chen, D. R. Clarke, S. H. Fan, K. E. Goodson, P. Keblinski, W. P. King, G. D. Mahan, and A. Majumdar, Appl. Phys. Rev. **1**, 011305 (2014).
[3] D. G. Cahill, W. K. Ford, K. E. Goodson, G. D. Mahan, A. Majumdar, H. J. Maris, R. Merlin, and S. R. Phillpot, J. Appl. Phys. **93**, 793 (2003).
[4] J. Pendry, J. Phys. Condens. Matter **11**, 6621 (1999).
[5] S. Shen, A. Narayanaswamy, and G. Chen, Nano Lett. **9**, 2909 (2009).
[6] S. Basu and M. Francoeur, Appl. Phys. Lett. **99**, 143107 (2011).
[7] S. J. Petersen, S. Basu, and M. Francoeur, Photonics Nanostruct. Fundam. Appl. **11**, 167 (2013).
[8] S.-A. Biehs, M. Tschikin, and P. Ben-Abdallah, Phys. Rev. Lett. **109**, 104301 (2012).
[9] C. Cortes, W. Newman, S. Molesky, and Z. Jacob, J. Opt. **14**, 063001 (2012).
[10] Y. Guo, C. L. Cortes, S. Molesky, and Z. Jacob, Appl. Phys. Lett. **101**, 131106 (2012).
[11] S. Molesky, C. J. Dewalt, and Z. Jacob, Opt. Express **21**, A96 (2013).
[12] R. Guérout, J. Lussange, F. S. S. Rosa, J.-P. Hugonin, D. A. R. Dalvit, J.-J. Greffet, A. Lambrecht, and S. Reynaud, J. Phys. Conf. Ser. **395**, 012154 (2012).
[13] J. Dai, S. A. Dyakov, and M. Yan, Phys. Rev. B **92**, 035419 (2015).
[14] X. L. Liu, B. Zhao, and Z. M. Zhang, Phys. Rev. A **91**, 062510 (2015).
[15] K. Park, S. Basu, W. P. King, and Z. M. Zhang, J. Quant. Spectrosc. Radiat. Transfer **109**, 305 (2008).
[16] K. Hoshino, A. Gopal, M. S. Glaz, D. A. Vanden Bout, and X. Zhang, Appl. Phys. Lett. **101**, 043118 (2012).
[17] C. R. Otey, W. T. Lau, and S. Fan, Phys. Rev. Lett. **104**, 154301 (2010).
[18] L. P. Wang and Z. M. Zhang, Nanoscale Micro. Thermophys. Eng. **17**, 337 (2013).
[19] Y. Yang, S. Basu, and L. P. Wang, Appl. Phys. Lett. **103**, 163101 (2013).
[20] P. Ben-Abdallah and S.-A. Biehs, Phys. Rev. Lett. **112**, 044301 (2014).
[21] Y. Yang, S. Basu, and L. P. Wang, J. Quant. Spectrosc. Radiat. Transfer **158**, 69 (2015).
[22] W. Gu, G. H. Tang, and W. Q. Tao, Int. J. Heat Mass Transfer **82**, 429 (2015).
[23] M. Lim, S. S. Lee, and B. J. Lee, Phys. Rev. B **91**, 195136 (2015).
[24] R. St-Gelais, B. Guha, L. Zhu, S. H. Fan, and M. Lipson, Nano Lett. **14**, 6971 (2014).
[25] K. Ito, A. Miura, H. Iizuka, and H. Toshiyoshi, Appl. Phys. Lett. **106**, 083504 (2015).
[26] H. Wang and L. Wang, Opt. Express **21**, A1078 (2013).
[27] B. Zhao, L. Wang, Y. Shuai, and Z. M. Zhang, Int. J. Heat Mass Transfer **67**, 637 (2013).
[28] H. Wang, Y. Yang, and L. Wang, Appl. Phys. Lett. **105**, 071907 (2014).
[29] H. Wang, Y. Yang, and L. P. Wang, J. Appl. Phys. **116**, 123503 (2014).
[30] H. Wang, Y. Yang, and L. P. Wang, J. Opt. **17**, 045104 (2015).
[31] L. P. Wang and Z. M. Zhang, Opt. Express **19**, A126 (2011).
[32] L. P. Wang and Z. M. Zhang, J. Opt. Soc. Am. B **27**, 2595 (2010).
[33] G. Bimonte, Phys. Rev. A **80**, 042102 (2009).
[34] R. Messina and M. Antezza, Europhys. Lett. **95**, 61002 (2011).
[35] M. Krüger, T. Emig, and M. Kardar, Phys. Rev. Lett. **106**, 210404 (2011).
[36] L. Li, J. Opt. Soc. Am. A **13**, 1870 (1996).
[37] M. G. Moharam, E. B. Grann, D. A. Pommet, and T. K. Gaylord, J. Opt. Soc. Am. A **12**, 1068 (1995).
[38] L. P. Wang, S. Basu, and Z. M. Zhang, J. Heat Transfer **134**, 072701 (2012).
[39] A. Lambrecht and V. N. Marachevsky, Phys. Rev. Lett. **101**, 160403 (2008).
[40] J. Lussange, R. Guérout, F. S. S. Rosa, J.-J. Greffet, A. Lambrecht, and S. Reynaud, Phys. Rev. B **86**, 085432 (2012).
[41] R. Guérout, J. Lussange, H. B. Chan, A. Lambrecht, and S. Reynaud, Phys. Rev. A **87**, 052514 (2013).
[42] See Supplemental Material at http://link.aps.org/supplemental/10.1103/PhysRevLett.117.044301 for validation of numerical calculations, comparison with proximity approximation method for the case without magnetic polariton, a brief discussion about effective medium approximation, comparison between metallic gratings and slits, and effect of grating misalignment.
[43] X. L. Liu and Z. M. Zhang, Appl. Phys. Lett. **104**, 251911 (2014).
[44] H. Chalabi, E. Hasman, and M. L. Brongersma, Phys. Rev. B **91**, 014302 (2015).
[45] X. L. Liu, T. J. Bright, and Z. M. Zhang, J. Heat Transfer **136**, 092703 (2014).